Nuclear Instruments and Methods in Physics Research A 387 (1997) 163–170

NUCLEAR INSTRUMENTS & METHODS IN PHYSICS RESEARCH Section A

ELSEVIER

Laterally resolved measurements of polycrystalline cesium iodide surfaces

Petra Rudolf[a], F. Marchal[a], R. Sporken[a], R. Caudano[a], Tiziana dell'Orto[b], J. Almeida[c], A. Braem[d], F. Piuz[d], S. Sgobba[d], G. Paic[e], E. Nappi[f], A. Valentini[f], P. Sartori[g], C. Coluzza[h,*]

[a] *LISE – Facultés Universitaires Notre-Dame de la Paix, Rue de Bruxelles 61, 5000 Namur, Belgium*
[b] *Centro di Competenza per la Microelettronica/Consorzio Roma, Richerche Via Orazio Raimondo 8, 00173, Roma, Italy*
[c] *Institute de Physique Appliquée, Ecole Polytechnique Fédérale de Lausanne, 1015 Ecublens, Lausanne, Switzerland*
[d] *CERN/Div. PPE, 1121 Geneva 23, Switzerland*
[e] *Subatech, Ecole des Mines 4, Rue A. Kastler, 44070 Nantes Cedex 03, France*
[f] *INFN, Sez. di Bari, Via Amendola 173, 70126, Bari, Italy*
[g] *INFN – Sez. di Padova, Dipartimento di Fisica "G. Galilei", Via Marzollo 8, 35121, Padova, Italy*
[h] *INFN – Sez. di Roma I, Dipartimento di Fisica "G. Marconi", P.le A. Moro 2, 00185, Roma, Italy*

Abstract

The aim of this work was to establish the correlation between the local chemical composition and morphology of polycrystalline cesium iodide (CsI) and its local quantum efficiency. We used a laterally resolved Electron Spectroscopy for Chemical Analysis (ESCA-300) apparatus and a Scanning Auger Microprobe (SAM) to investigate the lateral inhomogeneity of the CsI surface stoichiometry. The local quantum efficiency (QE) was determined by measuring the secondary electron emission in Photoemission Electron Microscopy both with a non-monochromatized deuterium lamp and with tunable X-ray synchrotron radiation as the excitation source. CsI films on different substrates were studied. We found that the local QE depends strongly on the morphology, on the local stoichiometry and on carbon contamination. The results allow for an optimisation of the quantum efficiency of large area photocathodes.

1. Introduction

Cesium iodide is one of the most efficient and widely used for UV and soft-X-ray converters [1–23]. However, very few studies [24–30] have dealt so far with the CsI surface chemical properties and their lateral homogeneity, a subject of utmost importance in optimizing such converters. The goal of our investigation was to compare its local chemical composition with the local quantum efficiency (QE) as derived from the secondary photoelectron emission. CsI deposited on different substrates and its modification by low temperature (50°C) thermal annealing were studied. Many of the chemical and physical processes on solid state surfaces are determined by the inhomogeneous nature of the material: in the case of a polycrystalline CsI surface the local morphology and the local differences in chemical state can influence the photoelectric threshold, the localized surface dipoles, the defects, and other factors that control the secondary electron yield, and therefore the QE. Spatially-integrated surface analysis techniques such as standard X-ray photoemission do not permit a deep clarification of such phenomena. Laterally resolved photoemission allows one to overcome this limit opening the way to a novel analysis methodology: the spectromicroscopy. The study of inhomogeneous materials such as polycrystalline surfaces, is a good example for the new frontiers in the measurements of local properties. Furthermore the lateral resolution is crucial in the study of insulators where local charging effects can easily induce artifacts in spatially integrated X-ray photoemission results [31]. Our study employed a laterally resolved Electron Spectroscopy for Chemical Analysis (ESCA-300) apparatus [32] and a Scanning Auger Microprobe (SAM) to investigate the lateral inhomogeneity of the surface stoichiometry of polycrystalline CsI films. To obtain the local quantum efficiency (QE) we measured the secondary electron photoemission by a Photoemission Electron Microscope both in PEEM mode (excitation by a non-monochromatized deuterium lamp) and in XSEM mode (excitation by tunable X-ray synchrotron radiation source) [33]. The results on the local chemical composition and the local QE were also compared to the film morphology determined by Scanning Electron Microscopy (SEM). These experiments revealed that it is possible to improve

* Corresponding author.

PII S0168-9002(96)00981-3

the QE by choosing the most suitable substrate to obtain an optimal uniformity in the morphology and the stoichometry of the film and by applying a soft annealing treatment. We also found that grain boundaries in the film are dead areas where the QE is zero and that carbon contamination strongly influences the QE.

2. CsI film preparation

Thin films (5000 Å) of CsI were grown by sublimation of either CsI (MERCK Art. 2861) or CsI monocrystals placed in molybdenum crucibles. The investigated substrates were copper, aluminum, stainless-steel, and substrates used in the production of standard printed circuits (G10). The G10 consists in a substrate of epoxy resin reinforced by fiber glass and covered by a conducting coating of Cu. A first series of depositions was made on G10 substrates, after chemical coating with an Au layer. The unsatisfactory quality of the CsI films on each substrates induced us to substitute the Au coating of G10 by the more effective coatings consisting either in a single layer of Sn or in a double layer of Au and Ni. The Ni coated G10 sample were electrochemically polished before depositing the Au layer. The substrate temperature was 22–25°C during the CsI deposition. Two quartz balances monitored the deposition rate. During CsI sublimation the pressure rose to $\approx 10^{-6}$ mbar (base pressure $\sim 10^{-7}$ mbar). After deposition, the samples were stored in stainless-steel boxes filled with nitrogen, and exposed to air only for a few minutes during the introduction in the ESCA-300 apparatus, the XSEM-PEEM, the SEM or the SAM apparatus which all operate in UHV. Some samples were activated in situ by annealing at 50°C for several hours [26] before the analysis.

3. CsI film characterization

Electron spectromicroscopy was performed using different excitation sources (electrons or photons at different energies) in order to study the local value of the QE (proportional to the integral of the secondary electrons emission curve) as a function of local stoichiometry and morphology.

In the left-hand panel of Fig. 1 we show PEEM images taken with the VUV deuterium lamp (continuous emission spectrum up to 6.7 eV) for CsI deposited on Au/G10 (a), on Sn/G10 (c) and on Au/Ni/G10 (e). In these PEEM experiments the VUV radiation excites secondary electrons at very low kinetic energies. The secondary emission microimages correspond to a QE mapping. By measuring the averaged pixel intensity, we discovered that CsI on Au/Ni/G10 produced a QE which was a factor of two higher than that of the films deposited on standard Au/G10, and close to the optimum value obtained on polished stainless-steel substrates. To gain information on the morphology of the films, SEM images were collected on the same samples with a LEICA Stereoscam 360 apparatus operating at a primary energy of the electrons of 20 keV and equipped with a Link microanalyser. The samples had to be coated with a 20 nm Au layer to enhance their surface conductivity, however, such a thin layer does not alter the surface morphology. The images relative to CsI on Au/G10 (b), on Sn/G10 (d) and on Au/Ni/G10 (f) are shown in the right-hand panel of Fig. 1. From the comparison of each of these images with the corresponding PEEM image, one sees immediately that many of the features in the PEEM image are related to the morphology determined by SEM. This demonstrates that the spatial variations of the QE depend on the local morphology of the film. In particular, it is evident that grain boundaries are a dead area from which no photoelectrons are emitted. To obtain the highest QE from a film it is therefore desirable to increase the grain dimension and, if possible, to use a monocrystalline layer. However, when we measured a monocrystalline sample, we found that the charging effect was so strong (CsI has a gap of about 6 eV) that it inhibited the emission of photoelectrons. N-doped monocrystalline samples could maybe overcome this problem.

In the PEEM images in Fig. 1 one can also identify large dark zones far away from any grain boundary. This indicates that not only the local morphology but also the local stoichiometry is a crucial parameter for the QE. To obtain chemical information with a spatial resolution similar to that used in the morphological studies [26–29] we moved to laterally-resolved ESCA and XSEM. In the ESCA measurements Al Kα X-ray photons (1486.7 eV) generated from a rotating anode are used for the excitation of secondary electrons and of photoelectrons from Cs 3d and I 3d core levels. The ESCA-300 system is described in [32]. Briefly, we worked with an energy resolution of 0.30 eV and a lateral resolution of 27 μm, as determined by resolving lithographic microstructures.

With ESCA we measured the lateral distribution of I and Cs studying the lateral variation of the 3d core level intensity for each element. The results are shown in Fig. 2 for a CsI film deposited on Al and annealed at 50°C, together with the secondary electron emission image taken on the same area. In all three images bright regions correspond to larger signal than the dark regions. Note that the 3d cross sections for the two elements are quite similar, therefore a higher intensity reflects a higher concentration of the corresponding element. The Cs and I distribution images of the unannealed samples (not shown) are similar, but we found that a soft annealing (less than 60°C) for few hours increases the secondary electron emission intensity.

In a different series of experiments synchrotron radiation ($h\nu < 100$ eV) was utilized for chemical imaging by generating the difference between Photoemission Electron Microscopy images taken below and above the Cs 4d or I 4d absorption edges (XSEM mode). The XSEM experi-

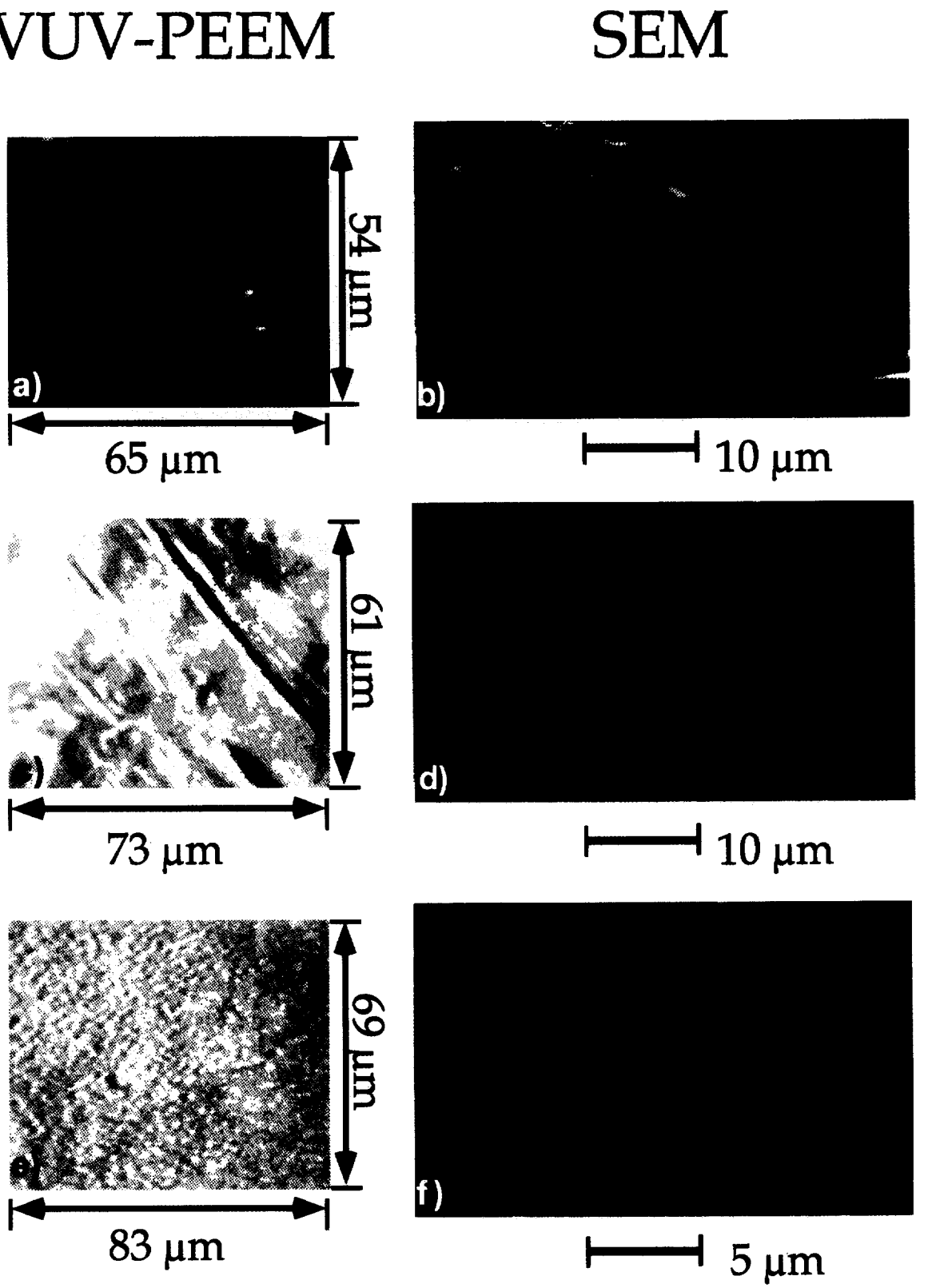

Fig. 1. Left-hand panel: VUV secondary emission microimages of QE fir CsI deposited on Au/G10 (a), Sn/G10 (c) and Au/Ni/G10 (e). Right-hand panel: SEM images of the same samples evidencing the local morphology: for CsI on Au/G10 (b), Sn/G10 (d) and Au/Ni/G10 (f).

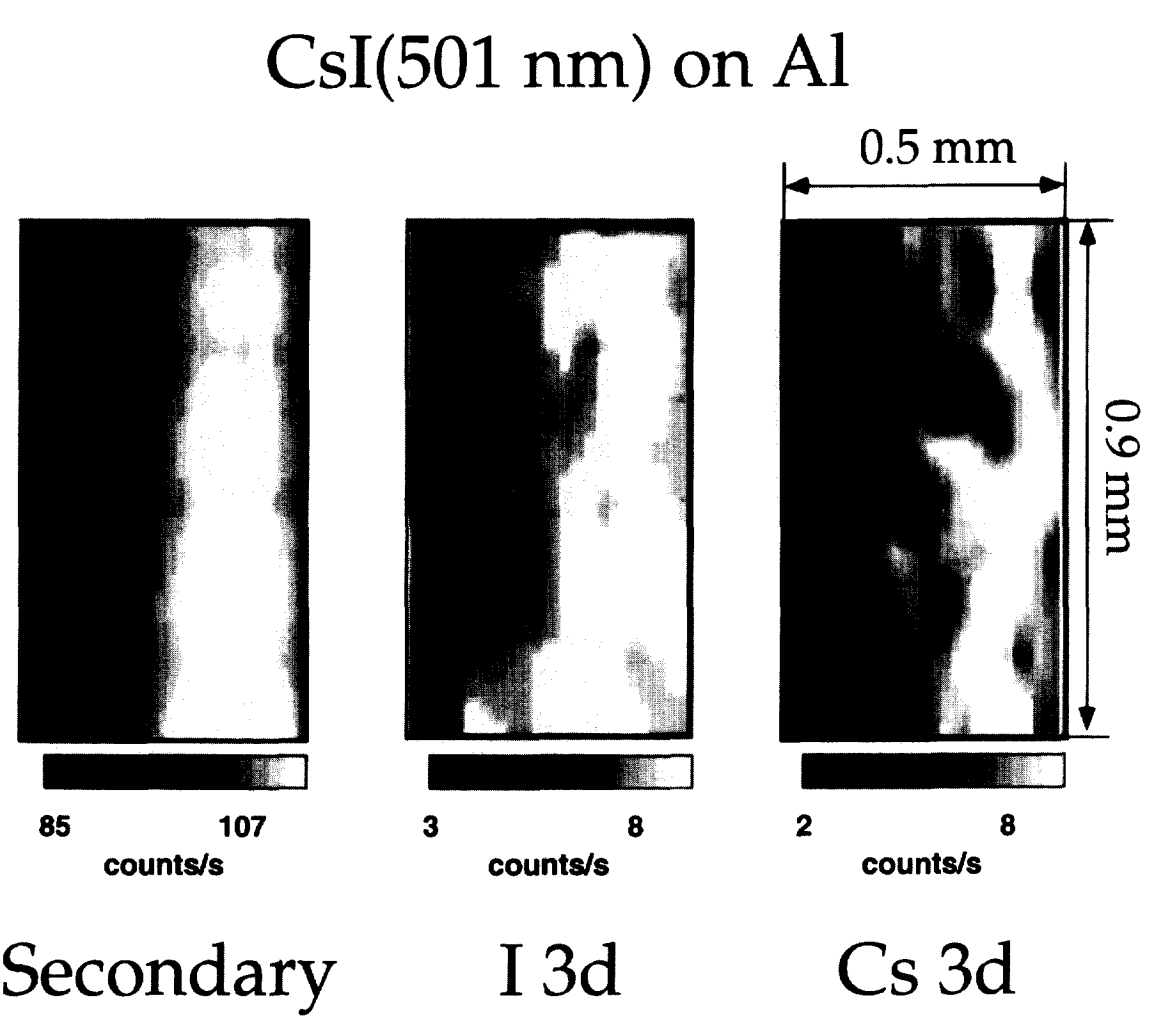

Fig. 2. Two-dimensional surface distribution by the spatially-resolved ESCA of the secondary electrons yield, of the I 3d core level intensity, and of the Cs 3d core level intensity, for a 0.5 mm thick CsI film on Al, after annealing at 50°C for 6 h. The bright regions correspond to larger signal than the dark regions.

ments were performed at the Wisconsin Synchrotron Radiation Center on the 3-meter toroidal-grating monochromator beamline, with the instrument described in [33]. The spatial resolution was ≈2 μm, determined in the same way as in the ESCA experiment. We obtained similar results at Elettra, the synchrotron radiation facility in Trieste. In this case the microscope was on an undulator beamline. Since the beamline was not equipped with a monochromator, the photon energy was tuned by changing the gap of the undulator. The photon energy resolving power was ~33, sufficient to discriminate the absorption edges of Cs and I. The microscope was also used in the PEEM mode in order to study the effects of different photon energies on the quantum efficiency. The results showed that the spatial inhomogeneities of the relative QE are not related to the energy of the exciting radiation we used, but they could be a function of the photon beam intensity [26].

The top panel in Fig. 3 shows PEEM image of the secondary electron emission and the XSEM micrographs of the Cs and I distributions on a CsI film deposited on Al after annealing at 50°C. Bright regions correspond to areas of stronger emission. The resolution was not sufficient to image individual CsI grains whose size (determined by SEM) was ≈1 μm, but the images show lateral variations on a scale of 10 μm or less. The Cs and I distributions were obtained by digital subtraction of XSEM images taken at photon energies above and below the Cs 4d or I 4d absorption edge. The signal intensities were normalized to the photon flux before the subtraction. Even a rough analysis of Figs. 2 and 3 shows that the areas of strongest signal in the secondary-electron image occur where the

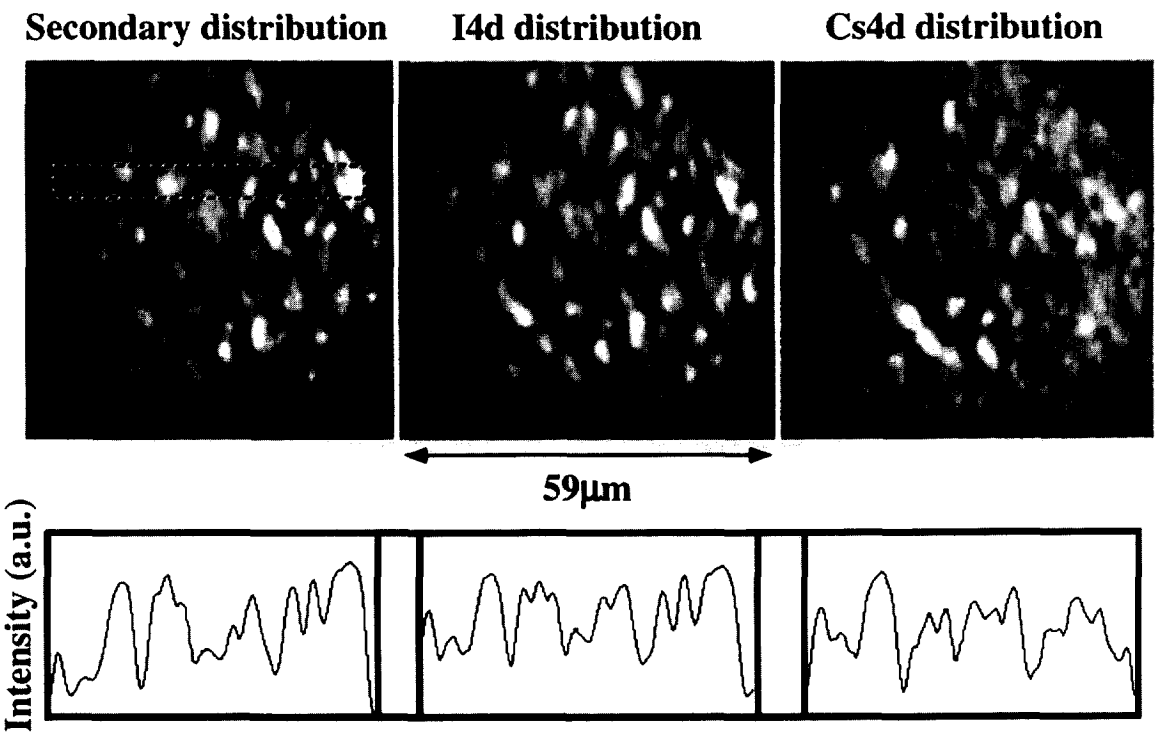

Fig. 3. Top panel: XSEM micrographs of 0.5 μm thick CsI film on Al, after annealing at 50°C for 6 h. The images correspond to the intensity distributions of secondary electrons (left), of the I 4d (center) and of the Cs 4d (right) photoelectrons. In the lower panel we show intensity profiles corresponding taken along the bar shown in the secondary electrons image.

intensity in the iodine image is highest. This correlation is more evident if one takes specific intensity scans across the images, such as those shown in the lower panel of Fig. 3. These scans were collected along the horizontal bar shown in the secondary-electron image and reveal that secondary electron emission follows quite well the intensity profile of the iodine signal. Similar results were obtained scanning over many different areas the sample. This finding is not unique to CsI on Al, in fact, for all other substrates except Cu we confirmed that iodine-rich surface areas yield the highest quantum efficiency. On the contrary, in the case of Cu substrates (not shown), we found that the QE was very low nearly all over the surface, but in the few spots were it was high we found only Cu and Cs. This behaviour can be explained by the chemical reaction between CsI and Cu giving rise to the formation of copper iodide, a compound which peels out from the substrate in form of black dust [28,29].

For a chemical analysis with higher spatial resolution Auger microimages were collected with a Scanning Auger Microprobe PHI 595, with a spatial resolution set to 2 μm, a primary energy of the e-beam of 7 keV, a current on the sample in the nanoampere range, and scanning in the image mode an area of about 1 mm^2. The SAM images shown in Fig. 4 represent the current emitted from the sample and can therefore be taken as a measurement of the secondary electron yield. For the as introduced samples (a), (b) and (c) one notices that the image is very uniform, and only a few slightly brighter or slightly darker areas can be identified on the surface if the contrast is pushed to the maximum. CsI deposition on Au/Ni/G10 substrates (Fig. 4(a)) and on polished stainless-steel substrates (Fig. 4(b)) seems to yield the highest uniformity, the CsI films on aluminum are a bit more contrasted than those on Au/Ni/G10 and polished stainless-steel. The CsI film on Cu substrates (Fig. 4(d)) shows instead clearly some non-uniformity characterized by lighter and darker stripes and the aged film (3 weeks in air) on Au/Ni/G10 (Fig. 4(e)) looks strongly contrasted.

Fig. 5 shows Auger spectra of different spots on the samples shown in the SAM images of Fig. 4: (a) is collected on a brighter area and (b) on a gray area of Au/Ni/G10 sample (see Fig. 4(a)); (c) and (d) refer to scans on a gray and black spot respectively of the aged G10/Ni/Au (see Fig. 4(e)) and (e) was recorded on a gray spot of the Cu substrate (see Fig. 4(d)). The area scanned in spectra acquisition mode is 1200 μm^2 for all samples, the e-gun parameters are the same as for the SAM images in Fig. 4. Comparing the spectra relative to bright and gray spots on the CsI on Au/Ni/G10, one notices that the

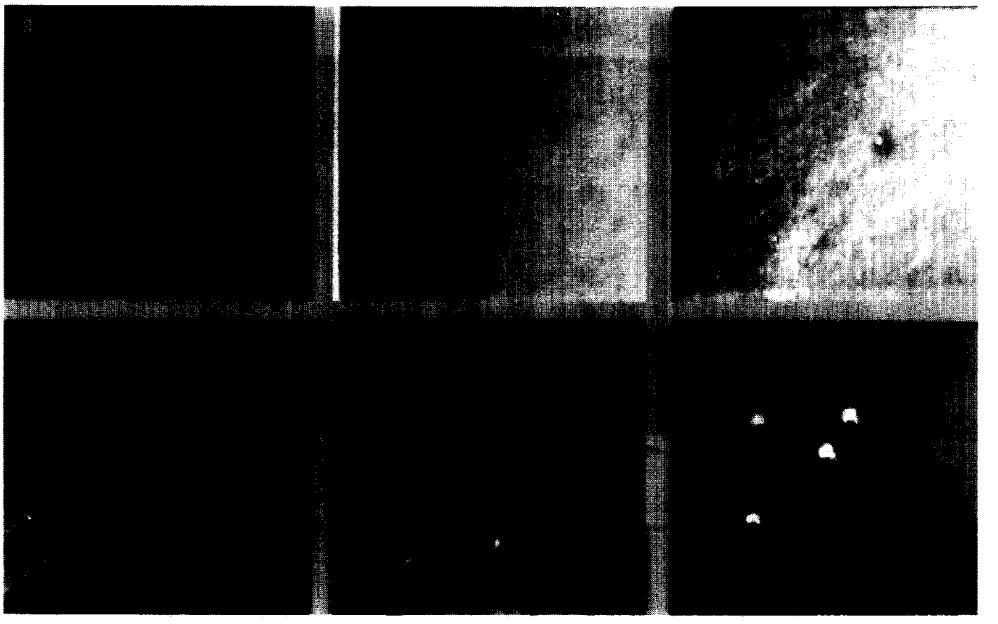

Fig. 4. Secondary electrons microimages of CsI deposited onv ariojs substrates: (a) on Au/Ni/G10 as introduced; (b) on polished stainless steel as introduced; (c) on aluminum as introduced; (d) on copper as introduced; (e) on Au/Ni/G10 after aging in air for 3 weeks; (g) on Au/Ni/G10 after collecting Auger spectra in different points.

slightly brighter areas correspond to C-contamination, while no chemical change is detectable for the slightly darker areas. The C-contamination disappears after the first spectra are collected (total of 5 min of acquisition). No substrate peaks are visible. The same observations are made also for polished stainless-steel and aluminum substrates. The aged CsI film on Au/Ni/G10 shows a stronger C-contamination than the vacuum stored CsI on Au/Ni/G10 and its brighter spots seem to contain less Cs; however no substrate peaks are seen after aging. The surface of the CsI on Cu instead is strongly O contaminated, the Cu peaks are clearly seen and iodine is not visible in this case (maybe masked by O peak or, in agreements with ESCA and XSEM results, due to the peel-out of the CuI compound). One can therefore conclude that while deposition on Au/Ni/G10, on polished stainless-steel, and on aluminum substrates leads to covering films exhibiting a uniform secondary electron yield, the deposition on Cu substrate leads to non-uniform growth, and CsI decomposition (Cs relative peak areas in the doublet differ from those on good substrates). One can also infer that aging does not break up the film if it was covering when freshly deposited. Moreover the secondary electron yield is slightly higher in C-contaminated areas than in clean areas. If one records another SAM image after acquiring spectra in certain points (see Fig. 4 (f)) the latter show up much brighter, indicating that the total removal of the C-contamination greatly enhances the secondary electron yield. We tried to electron desorb the C-contamination by scanning the sample in the image mode for 1 h, but this treatment gives rise to only a slight decrease in the C signal and causes no significant increase of the local QE. One possible explanation is that the increase in secondary electron yield is not an electron induced effect, but due to sample heating since the power on the reduced area in the spectra acquisition mode is about 1600 times higher than that in the image mode. Alternatively, the increase in secondary electron yield could be related not only to the removal of the C-contamination but also to the density of defects created on the surface through electron bombardment and this defect density will increase with the power like the sample heating.

4. Summary

We have studied how the lateral variation in the QE of CsI films on different substrates depends on the local chemical properties of the films, which in turn are influenced by the morphology. For all substrates except Cu, we found iodine-rich parts of the surface showed a higher QE and that the grain boundaries are dead areas for photoemission of secondary electrons. The best QE values were obtained for CsI deposited on Au/Ni/G10 and were similar to the best values reported in literature for CsI on polished stainless-steel. These films had the most uniform surface morphology and were resistant to aging. We also discovered that the carbon surface contamination lowers the local quantum efficiency. Due to the chemical reaction

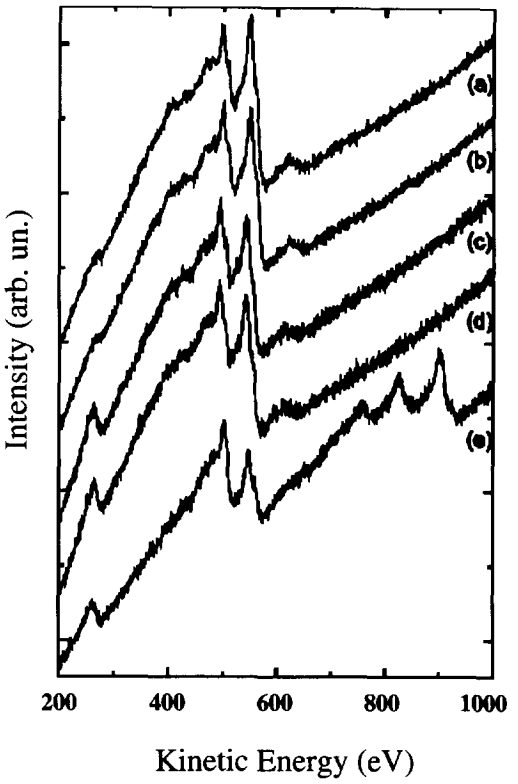

Fig. 5. Auger spectra of different spots on the samples shown in Fig. 4: (a) is collected on a brighter area and (b) on a gray area of CsI on Au/Ni/G10 substrate as introduced; (c) and (d) refer to scans on a gray and a black spot respectively of the aged CsI on Au/Ni/G10; (e) was recorded on a gray spot of the CsI on coper substrate.

of CsI with Cu which results in CuI formation, on Cu-substrates the QE is in general much lower and in the few small regions with high QE we found only Cu and Cs.

Acknowledgements

We thank B.P. Tonner, Gelsomina De Stasio, F. Barbo, M. Bertolo, A. Binco, S. Cerasari, S. Fontana, T. Scognetti, H. Jotterand and Pierre Louette for their technical and scientific support, and G. Margaritondo and A. Breskin for helpful discussions. We acknowledge support from the National Fund for Scientific Research (Belgium). This work is supported by the Walloon Region and by the Belgian Federal Services for Scientific, Technical and Cultural Affairs (Interuniversity Attraction Poles on "Science of Interfaces and Mesoscopic Systems" and on "Material Characterization"), by the Belgian National Fund for Collective Research, by Italian National Institute for Nuclear Physics, and by CERN Research and Development Project RD26.

References

[1] B.L. Henke, J.A. Smith and D.T. Attwood, J. Appl. Phys. 48 (1977) 1852.
[2] B.L. Henke, J. Liesegang and S.D. Smith, Phys. Rev. B. 19(6) (1979) 3004.
[3] B.L. Henke, J.P. Knauer and K. Premaratne, J. Appl. Phys. 52 (1981) 1509.
[4] S.A. Schwarz, J. Appl. Phys. 68 (1990) 2382.
[5] G.W. Fraser, Nucl. Instr. and Meth. 206 (1983) 251.
[6] G.W. Fraser, Nucl. Instr. and Meth. 206 (1983) 265.
[7] J. Séguinot, G. Charpak, Y. Giomataris, V. Peskov, J. Tischauser and T. Ypsilantis, Nucl. Instr. and Meth. A 297 (1990) 133.
[8] D.C. Imrie, A.H. Moghul, K. Wells, G. Charpak and V. Peskov, Nucl. Instr. and Meth. A 310 (1991) 122.
[9] D.F. Anderson, S. Kwan and V. Peskov, Nucl. Instr. and Meth. A 326 (1993) 611.
[10] H. Bräuning, A. Breskin, R. Checkik, P. Miné and D. Vartsky, Nucl. Instr. and Meth. A 327 (1993) 369.
[11] A. Akkerman, A. Gibrekhterman, A. Breskin and R. Chechik, J. Appl. Phys. 72 (1992) 5429.
[12] A. Akkerman, A. Breskin, R. Chechik and A. Gibrekhterman, Secondary electron emission from alkali halides induced by X-rays and electrons, presented at the NATO Advanced Research Workshop on Ionization of Solids by Heavy Particles, Taormina, Italy, June 1992.
[13] A. Breskin, R. Chechik, V. Dangendorf, S. Majewski, G. Malamud, A. Pansky and D. Vartsky, Nucl. Instr. and Meth. A 310 (1991) 57.
[14] G. Melchart, G. Charpak, F. Sauli, G. Petersen and J. Jacobe, Nucl. Instr. and Meth. 180 (1981) 613.
[15] V. Dangendorf, A. Breskin, R. Chechik and H. Schmidt-Böcking, Nucl. Instr. and Meth. A 308 (1991) 519.
[16] A. Breskin and R. Chechik, Nucl. Instr. and Meth. 227 (1984) 24.
[17] G.W. Fraser, M.A. Barstow, J.F. Pearson, M.J. Whitely and M. Lewis, Nucl. Instr. and Meth. 224 (1984) 272.
[18] J.E. Bateman and R.J. Apsimon, Adv. Elec. Phys. 52 (1979) 189.
[19] A. Akkerman, A. Breskin, R. Chechik, V. Elkind, A. Gibrekhterman and S. Majewski, Nucl. Instr. and Meth. A 315 (1992) 82.
[20] A. Akkerman, A. Breskin, R. Chechik, V. Elkind, I. Frumkin and A. Gibrekhterman, Ultrafast secondary emission 2D X-ray imaging detectors, Proc. European Workshop on X-ray Detectors for Synchtron Radiation Sources, Aussois, France, September 1991, ed. A.H. Walenta.
[21] D.F. Anderson, S. Kwan, V. Peskov and B. Hoeneisen, Nucl. Instr. and Meth. A 323 (1992) 626.
[22] G. Charpak, V. Peskov and D. Scigocki, Proc. Symp. on Particle Identification at High Luminosity Hadron Colliders, Fermilab, Batavia, 5–7 April 1989, p. 295.
[23] A.N. Beltsy, G. Comtet, G. Dujardin, A.V. Gektin, L. Hellner, I.A. Kamenskikh, P. Martin, V.V. Mikhailin, C. Pedrini and A.N. Vasil'ev, J. EL. Spec. and Rel. Phen. 80 (1996) 109.
[24] C. Coluzza and R. Moberg, Surf. Rev. and Lett. 2 (1995) 619.
[25] G. De Stasio, T. dell'Orto, F. Gozzo, D. Alfè, M. Bertolo, S. Fontana, M.T. Ciotti, D. Mercanti, C. Coluzza, P. Perfetti and G. Margaritondo, Synchrotron Radiation News 7 (1994) 18.

[26] C. Coluzza, G. Almeida, H. Berger, L. Perez, G. Margaritondo, A. Braem, F. Piuz, G. Paic, A. Di Mauro and E. Nappi, Nucl. Instr. and Meth. A 343 (1994) 152.

[27] J. Almeida, H. Berger, A. Bream, C. Coluzza, A. Di Mauro, A. Ljubicic Jr., E. Nappi, G. Margaritondo, G. Paic, F. Piuz, F. Posa, R. Ribeiro, T. Scognetti and D. Williams, Nucl. Instr. and Meth. A 348 (1994) 216.

[28] J. Almeida, F. Barbo, M. Bertolo, A. Bianco, A. Braem, S. Cerasari, C. Coluzza, Tiziana dell'Orto, S. Fontana, G. Margaritondo, E. Nappi, G. Paic, F. Piuz, R. Sanjines, T. Scognetti and S. Sgobba, Nucl. Instr. and Meth. A 361 (1995) 524.

[29] T. dell'Orto, J. Almeida, E. Conforto, C. Coluzza, G. Margaritondo, G. Paic, A. Braem, F. Piuz and B.P. Tonner, J. Vacuum Sci. Technol. A13 (1995) 2787.

[30] H. Berger, P. Besson, Ph. Bourgeois, A. Braem, A. Breskin, A. Buzulutskov, R. Checkik, E. Chesi, C. Coluzza, R. Ferreira-Marques, J. Friese, A. Gillitzer, H.A. Gustafsson, W. Hejny, J. Homolka, W. Kuehn, A. Ljubicic Jr., P. Maier Komor, G. Malamud, G. Margaritondo, R. Martinelli, A. Di Mauro, Ph. Miné, E. Nappi, R. Novotny, A. Orkarsson, G. Paic, F. Piuz, A. Policarpo, F. Posa, L. Peruzzo, R.S. Ribeori, S. Riess, J.C. Santiard, P. Sartori, G. Sartori, J. Schukraft, T. Scognetti, S. Sgobba, O. Svensson, T. Tustonic, A. Valentini, D. Vartsky, G. Vasileiadis, F. Di Venere and K. Zeitelhack, Nucl. Instr. and Meth., to be published.

[31] C. Coluzza, J. Almeida, Tiziana dell'Orto, F. Gozzo, P. Almeras, H. Berger, D. Bouvet, M. Dutoit, S. Contarini and G. Margaritondo, J. Appl. Phys. 76 (1994) 3710.

[32] U. Gelius, B. Wannberg, P. Baltzer, H. Fellner-Feldegg, G. Carlson, C.G. Johansson, J. Larson, P. Münger and G. Vegefors, J. Electron Spectrosc. Relat. Phenom. 52 (1990) 747.

[33] B.P. Tonner, G.R. Harp, S.F. Korand and Zhang, Rev. Sci. Instr. 63 (1992) 564.

[34] C. Coluzza, Nucl. Instr. and Meth., to be published.